DOI https: //doi. org/10.1007/s11595-018-1789-9

Syntheses and Evaluations of CdS with Various Morphologies for Photocatalytically Reducing CO_2

YANG Xiaoxiao[1], XIN Weiyue[2], YIN Xiaohong[1*], SHAO Xiao[1]

(1.Tianjin Key Laboratory of Organic Solar Cells and Photochemical Conversion, School of Chemistry and Chemical Engineering, Tianjin University of Technology, Tianjin 300384, China; 2. School of Chemical Engineering, East China University of Science and Technology, Shanghai 200237, China)

Abstract: A series of CdS with various shapes of microsphere, flower-like and leaf-like were template-freely synthesized by a hydrothermal method. Powder X-ray diffraction (XRD), Brunauer-Emmett-Teller (BET), scanning electron microscopy (SEM) and UV-vis absorption spectroscopy (UV-vis) were applied to characterize the morphology, optical and other physical properties of the as-prepared CdS. An optical spectrum analyzer was used to measure the wavelength of the illuminant on the slurry in the activity evaluations of photocatalytic reduction of CO_2 over CdS. Both sources of cadmium and sulfur had great impact on the CdS morphology as can be seen in the SEM images. By means of a series of activity evaluations, the microspheric CdS made from cadmium nitrate and thioacetamide showed better photocatalytic activity for the reduction of CO_2 to methyl formate (MF) in methanol than the flower-like and leaf-like CdS catalysts.

Key words: CdS; morphology; photocatalytic reduction; CO_2; methyl formate

1 Introduction

With the booming of the industry and economy, environmental issues have aroused wide public concern. Specially, the global warming is severe. Many measures have been accepted to solve the problems such as cutting use of fossil fuels, promoting clean energy stoves, and converting CO_2 to useful resources. Because of its thermodynamic stability CO_2 is greatly difficult to be reduced.

Till now, TiO_2 has been broadly studied for its photocatalysis since it is inexpensive and easily obtained. Many efforts have been paid to modify TiO_2 for enhancing the photocatalytic reduction rate of CO_2, including metal loading[1,2], nonmetal doping[3], usage of a high surface area substrate[1], *etc*. Zhao *et al* used methanol as a hole scavenger and sliver-modified TiO_2 (Ag-TiO_2) nanocomposite as catalyst, photocatalytically producing hydrogen and CO, CH_4 from CO_2 and water[4]. Sulfide with narrower band gap and color enhanced sunlight absorption has drawn many researcher's attention in photocatalytic reduction of CO_2. Chen *et al* reported that CO_2 was photocatalytically reduced to methyl formate in methanol by using ZnS and Ni-doped ZnS[5]. Jiang *et al* used $CdIn_2S_4$ as a photocatalyst for selectively reducing CO_2 to methyl formate in methanol under UV light irradiation[6]. The above papers have explored composite catalysts and multiple catalysts, while in this paper we focus on the morphological influence of single compound on the photocatalytic reduction of CO_2.

CdS, a semiconductor with band gap of 2.42 eV and excellent photoelectric conversion performance, has been used for the degradation of organic dyes[7], waste water treatment, and photocatalytic hydrogen production[8]. But used for photocatalytically reducing CO_2, CdS is still of great challenge. CdS could be synthesized by many methods, such as solid state reaction[9], hydrothermal method[10,11], hot colloidal method[12,13] and so on. Meanwhile, CdS catalysts with triangular-like shape, nanorods, multipods[14], and prickly spheres were already synthesized.

Our paper is unique in transforming different sulfur (S) sources and cadmium (Cd) sources to various morphologic CdS by hydrothermal synthesis and proposing the formation mechanism of photocatalytic reactions.

(Received: Dec. 15, 2016; Accepted: Oct. 14, 2017)

YANG Xiaoxiao(杨晓晓): E-mail:xiaoya911028@sina.com

* Corresponding author: YIN Xiaohong (尹晓红): Prof.; PhD;E-mail:yinxiaohong@tjut.edu.cn

Funded by the National Natural Science Foundation of China (Nos. 21176192 and 21776220)

2 Experimental

2.1 Preparation of catalysts

All of the chemical reagents such as cadmium dichloride ($CdCl_2·2.5H_2O$, CadD for short), cadmium nitrate ($Cd(NO_3)_2·4H_2O$, CadN for short), cadmium acetate ($Cd(CH_3COO)_2·2H_2O$, CadA for short), thioacetamide (TAA for short), thiourea (TU for short) were of analytical purity and used without further purification.

The CdS powders were prepared by the hydrothermal synthesis method. The procedure was: firstly, 5 mmol cadmium source (CadD, CadN, CadA) and 10 mmol TAA were dissolved in 45 mL deionized water under magnetic stirring until they were completely dissolved. The obtained transparent solution was moved into a 75 mL Teflon-lined stainless steel autoclave and sealed. Then the autoclave was maintained in an oven at 160 ℃ for 24 h. Afterwards, the autoclave was naturally cooled down to the room temperature. Finally, the deep yellow precipitate was washed with ethyl alcohol and deionized water three times respectively, and dried at 80 ℃ for 8 h. The temperature of hydrothermal synthesis was changed from 120 to 190 ℃, for the time of 4, 8, 24, 48 h. For sulfur source of TU, the dosage was changed to 15 mmol.

2.2 Characterization

The prepared CdS powders were investigated by a powder X-ray diffractometer (Cu Kα X-ray radiation) at a scanning speed of 2^{o} min^{-1}. The morphology and size were observed by a field emission scanning electron microscope (FE-SEM, JEOL-JSM6700F). BET of APP V-Sorb was used to measure the surface area, and the UV-vis diffuse reflection spectra were recorded on a Shimadzu UV-2550 spectrometer using $BaSO_4$ as the reference.

2.3 Photocatalytic activity

The photocatalytic activity of the CdS was assessed by the photocatalytic reduction of CO_2. The reaction occurred in a quartz reactor with a window exposing to the light and two circulating water interfaces, and also two connectors for inletting CO_2. The reaction temperature was controlled at 20±3 ℃ by using a thermostatic water bath. A UV lamp of 365 nm (measured by an optical spectrum analyzer, UPRtek MK350) and 250 W was used for solar simulator ultraviolet irradiation. 20 mg of photocatalyst and 20 mL of methanol were added into the reactor. CO_2 was bubbled through the slurry of photocatalyst and methanol at a flow rate of 200 mL/min for 30 min under a magnetic stirring. Then the reactor was sealed, and the lamp was turned on. 6 h later, the clear solution was separated centrifugally from the slurry and analyzed by a gas chromatography (SCION 456-GC) equipped with a hydrogen flame detector (FID). Blank tests were carried out by changing CO_2 to Ar or in dark and keeping the other conditions unchanged.

3 Results and discussion

3.1 XRD analysis of CdS catalysts

The crystal phase and morphology were characterized by XRD and SEM. Fig.1(A) shows the XRD patterns of the CdS catalysts prepared by using TAA as sulfur source, CadA, CadD, CadN as cadmium sources, respectively. The XRD patterns of using TU instead of TAA are exhibited in Fig.1(B). The XRD patterns were in good accordance with CdS (JCPDS:41-1049) and there were no other high peaks of impurity-phase to be detected. And we could also speculate from the spike in the XRD patterns that the crystalline of the CdS catalyst was well enough. As can seen be in the SEM images, the habits of the crystals seemed better, and the particle diameters were larger.

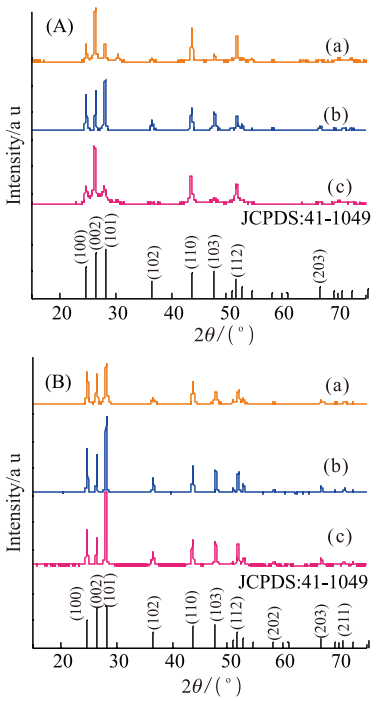

Fig.1 (A) XRD patterns of the CdS samples synthesized by using TAA as sulfur source; (B) XRD patterns of the CdS samples synthesized by using TU as sulfur source: (a) CadA sample, (b) CadD sample, (c) CadN sample

3.2 BET analysis

The BET specific surface areas of the CdS samples were calculated as shown in Table 1. The samples in Table 1 were synthesized using TAA and TU as sul-

Table 1 Surface area of the CdS samples synthesized by using TAA and TU as sulfur sources

Photocatalyst	CdS (CadA,TAA)	CdS (CadD,TAA)	CdS (CadN,TAA)
BET specific surface area/(m^2/g)	14.7	1.1	7.7
Photocatalyst	CdS (CadA,TU)	CdS (CadD,TU)	CdS (CadN,TU)
BET specific surface area/(m^2/g)	1.5	1.6	3.0

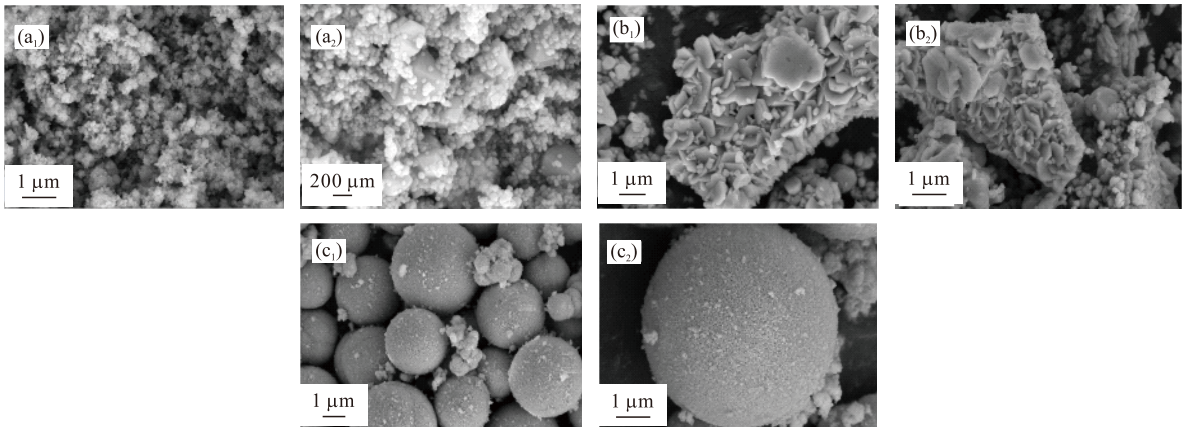

Fig.2 SEM images of CdS samples synthesized by using TAA as sulfur source:(a_1-a_2) CadA sample; (b_1-b_2) CadD sample; (c_1-c_2) CadN sample

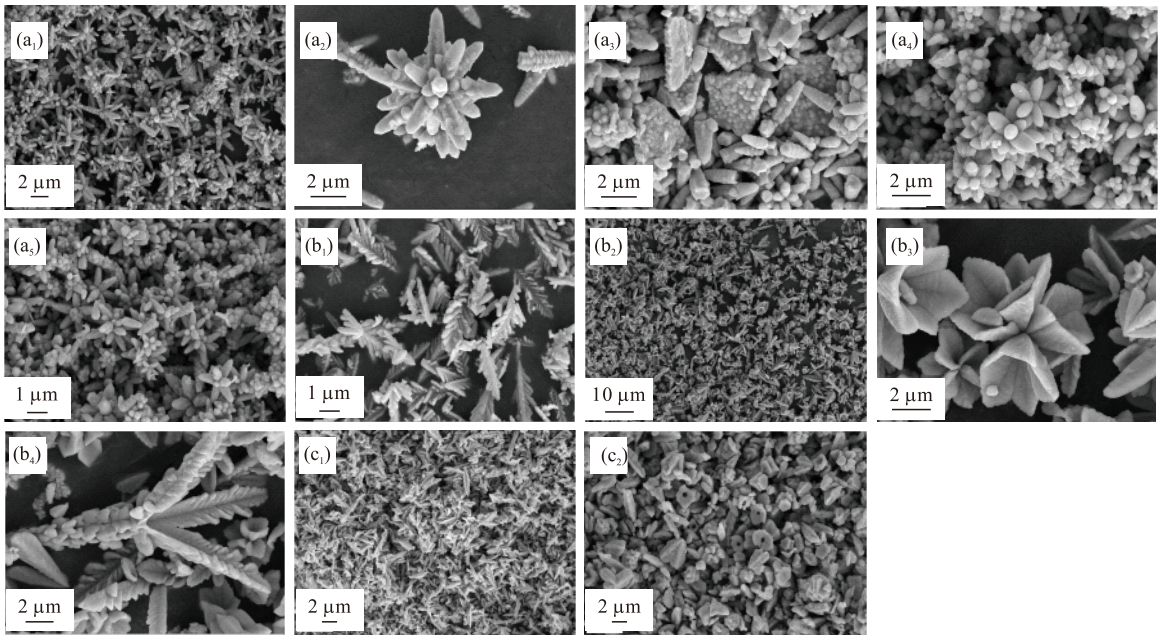

Fig.3 SEM images of CdS samples synthesized by using TU as sulfur source:(a_1-a_5) CadA sample; (b_1-b_4) CadD sample; (c_1-c_2) CadN sample

fur sources. It was obviously seen that the CdS synthesized from CadA had the largest surface area. The CdS samples using TU as sulfur source all had small specific surface areas. Although the morphologies of CdS samples made from TU were unique, it was unfavorable to increase the specific area because of the large scale of the catalyst particles (2-6 μm).

3.3 SEM analysis of CdS samples

Various shapes of the CdS samples were obtained by SEM as shown in Fig.2 and Fig.3. Figs.2(a)-(c) refer to the samples synthesized hydrothermally at 160 ℃ for different crystallization time, with TAA providing S^{2-} and CadA, CadD, CadN offering Cd^{2+} respectively. Other things being equal, by substituting TAA with TU, a series of other CdS morphologies were viewed (Figs.3(a)-(c)). Sulfur source played a big part in controlling the morphology of the catalysts by comparing the two sets of pictures mentioned above. When TAA served as sulfur source, CadA providing Cd^{2+}, CdS consisted of irregular nanoscale particles (Fig.2(a_1)).

With increasing crystallization time, the particle size distribution got more non-uniformity as can be seen in Fig.2(a_2). This nanoscale morphology made the samples have bigger surface areas as can be verified in Table 1. Replacing CadA with CadD, CdS was assembled by many small and irregular nanosheets (Figs.2(b_1)-(b_2)). By turning CadA into CadN, CdS microspheres (sizes ranging from 1 to about 6 μm) were synthesized (Fig.2(c_1)). Further observing the microspheres, they were not smooth but composed by a good deal of nano-granules (Fig.2(c_2)). CdS morphology was manifold as TU furnishing S^{2-} (Figs.3(a_1)-(c_2)). It was evidently found that kinds of flower-like CdS products were generated when CadA acted as cadmium source (Figs.3(a_1)-(a_5)). Most of the flowers were made up of several radially arranged rod-like petals (Figs.3(a_1)-(a_2)). The effects of crystallization time on the morphology of CdS seemed very significant. As shown in Fig.3(a_3)-Fig.3(a_5), with the increase of crystallization time, flowers were decreased changing into the mixture of sheets and rods (Fig.3(a_3)). As the crystallization time went further, sheet-like CdS microstructure disappeared and CdS products became flower structure with smaller size (Figs.3(a_4)-(a_5)). By using CadD as cadmium source (other conditions remained unchanged), the morphology of CdS was greatly different from that using CadA as cadmium source (Figs.3(b_1)-(b_4)). As shown in Fig.3(b_1), when the crystallization time was 4 h, all the morphology of CdS was leafy and each of the leaves was grown along a line symmetrically. With the crystallization time increased to 48 h (Figs.3(b_2)-(b_4)), leaves changed into the flowers in a variety of shapes such as hexapetalous flowers which were different from those shapes mentioned earlier. Figs.3(c_1)-(c_2) show the morphology of CdS taking CadN as cadmium supply. Within a short crystallization time, the morphology was like slender leaf (Fig.3(c_1)). The morphology became mussy when the crystallization time got longer as shown in Fig.3(c_2). According to the analyses above, it could be clearly seen that sulfur source, cadmium source and crystallization time all had crucial impacts on the synthesis of CdS with various morphologies.

3.4 Optical absorption properties of the CdS catalysts

The optical properties of CdS samples were studied by UV-vis spectroscopy. Fig.4 and Fig.5 displayed the UV-visible absorption spectra of CdS microparticles using TAA and TU as sulfur sources separately. All the samples clearly show strong absorption in the visible-light region as in Fig.4(A) and Fig.5(A). In theory, with the increase of the absorption intensity, the generation rate of electron-hole pairs on the catalyst surface increased, thereby promoting the photocatalytic reaction rate. The band gaps of the CdS samples were estimated by the equation of $ahv=A(hv-Eg)^{n/2}$, where hv was the photon energy, E_g was the band gap energy,

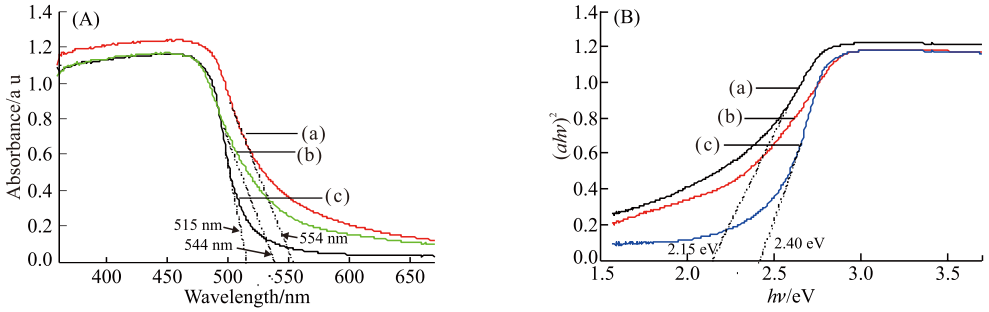

Fig.4 (A) UV-vis absorption of the different CdS samples synthesized by TAA as sulfur source: (a) CadN sample; (b) CadD sample; (c) CadA sample; (B) $(\alpha hv)^2$ *versus* the photon energy of CdS samples: (a) CadN sample; (b) CadD sample; (c) CadA sample

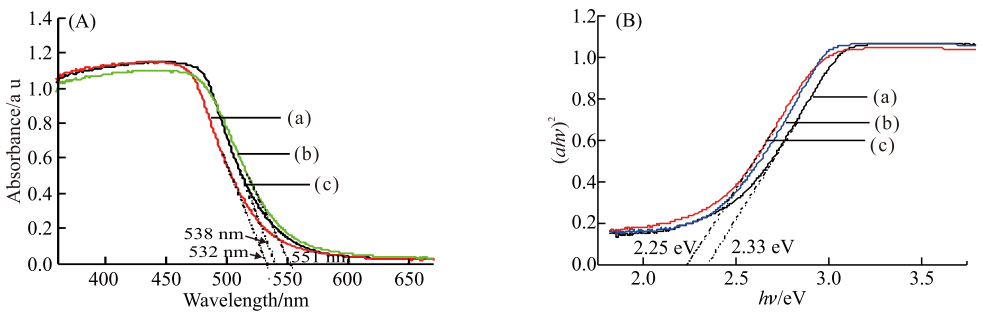

Fig.5 (A) UV-vis absorption of the different CdS samples synthesized by using TU as sulfur source: (a) CadN sample; (b) CadD sample; (c) CadA sample; (B) $(\alpha hv)^2$ *versus* the photon energy of CdS samples: (a) CadN sample; (b) CadD sample; (c) CadA sample

α was the absorption coefficient, and A was a constant relative to the material. Moreover, n was either 1 (for a direct transition) or 4 (for an indirect transition), which depended on the type of the transition in a semiconductor[15,16]. As can be seen from Fig.4(B) and Fig.5(B), the band gaps of the CdS samples were in the range of 2.15-2.40 eV. All the absorption of CdS samples showed a red shift compared to the typical band gap of the CdS crystal (2.42 eV). Generally speaking, red shift might be influenced by many factors such as particle size, morphology, size distribution, charge density *etc*[17].

3.5 Photocatalytic activity

The photocatalytic activity of the obtained CdS products was tested by the reduction of CO_2 in methanol under UV irradiation. Fig.6 shows the effects of different cadmium sources on the photocatalytic activity. The samples were all hydrothermally obtained at 160 ℃ for 24 h. It could be seen that when TAA was sulfur source, the sample made from CadN showed the highest activity and this might be attributed to its microsphere morphology (the morphology of the other two were chaotic) as can be seen in Figs.2(a)-(c). The increase of BET surface areas was conducive to improve the photocatalytic activity of catalysts[18]. Meanwhile, the catalystic activity of CadA sample was the weakest, which could be that the active points were covered. Thus, it could be seen that cadmium source played a great role in photocatalytic activity of CO_2 reduction. When TU acted as sulfur source, the sample synthesized from CadD had the best photocatalytic activity, while the activity of CadN sample was the worst. The influence of crystallization time on the photocatalytic activity was also investigated as shown in Fig.7, taking the CadN sample synthesized at 160 ℃ as an example. With the increase of crystallization time, the catalytic activity was enhanced first and then weakened. When the crystallization time was around 24 h, the catalysts showed better activity. In general, the samples taking TAA as sulfur source showed better photocatalytic activity. It should be highlighted that the two products MF and dimethoxymethane (DMM) were detected in methanol only by using the catalyst samples synthesized from CadN and TAA. As it could be seen from Fig.8, the yield of DMM was much lower than that of MF.

In order to explore the mechanism in the process, a serious of control groups were carried out. Control groups were mainly used to investigate the three CdS catalysts made from CadA, CadD and CadN, using TAA as sulfur source at 160 ℃ for 24 h. First, we made the photocatalytic reaction under irradiation in Ar atmosphere. As we could see in Table 2, MF was still tested in methanol, however, the yield was much lower than that in CO_2 atmosphere, indicating that MF was

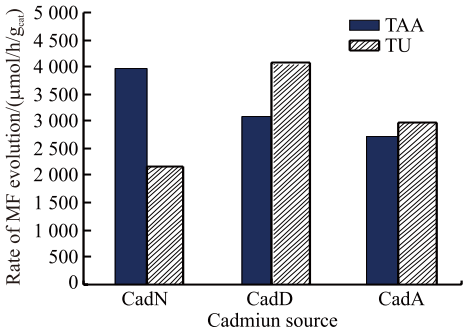

Fig.6 Photocatalytic activity of CdS samples synthesized by using different cadmium sources and different sulfur sources (T=160 ℃; t=24 h)

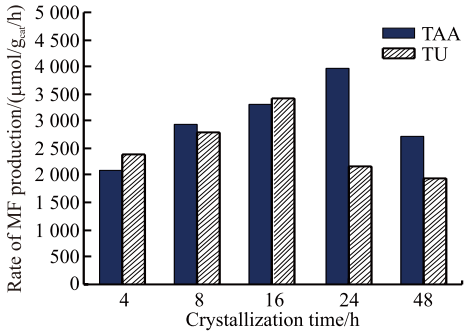

Fig.7 Photocatalytic activity of CdS samples synthesized using different sulfur sources and for different crystallization time (CadN served as cadmium source; T=160 ℃)

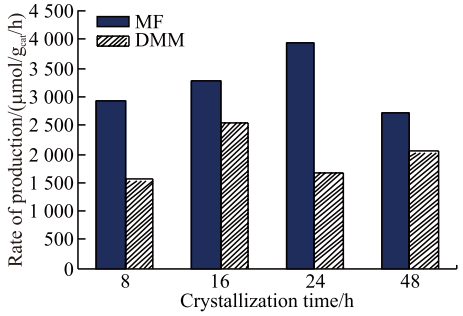

Fig.8 Photocatalytic activity of CdS samples synthesized from CadN and TAA for different crystallization time

Table 2 Rate of MF evolution in methanol under different conditions over CdS catalysts at 160 ℃ for 24 h

Samples	CdS (CadA, TAA)	CdS (CadD, TAA)	CdS (CadN, TAA)
Light, CO_2 yield of MF/ (μmol/h/g_{cat})	2 693.97	3 076.82	3 951.89
Light, Ar yield of MF/ (μmol/h/g_{cat})	1 058.54	1 173.39	1 304.65
Dark, CO_2 yield of MF/ (μmol/h/g_{cat})	0	0	0

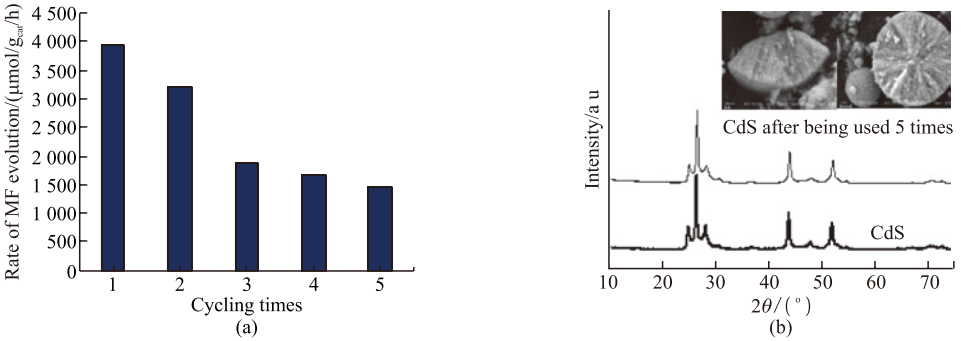

Fig.9 Cycling runs of CdS (CadN, TAA) catalyst under UV light irradiation for 10 h and XRD patterns, SEM images of CdS (CadN, TAA) catalyst before and after being used 5 times

mainly generated in the presence of CO_2. And then the control experiment in the dark with other conditions unchanged was also conducted (Table 2). MF was not detected meaning that the process was a photo-stimulated reaction.

3.6 Stability evaluation of the CdS samples

The stability of the CdS catalysts was evaluated by the successive uses in the process of photocatalytic reduction of CO_2. The sample used in stability evaluation was CdS made from CadN and TAA at 160 ℃ for 24 h. After each evaluation test, the CdS catalyst was recollected by centrifugation, and then reused without further treatment. As shown in Fig.9(A), the CdS catalysts could be reused for at most 2 times. With increasing recycle number, the activity of CdS exhibited significant loss, which demonstrated that the pure CdS was not photo-stable just as mentioned in many reports. Furthermore, in order to know the changes of CdS catalyst, XRD analyses of the CdS catalyst before and after being used five times are shown in Fig.9(B). The XRD patterns did not show obvious peak changes, however, the morphology of the microsphere CdS changed a lot as can be seen in the insets in Fig.9(B). The microspheres turned into broken ones, demonstrating the instability of CdS under the UV irradiation of the same extent.

3.7 Photocatalytic mechanism

The reaction mechanism of photocatalytic reduction of CO_2 to MF in methanol was summed up. Under ultraviolet radiation, the CdS catalysts could be easily excited creating photo-generated electron-hole pairs[19]. A portion of the electrons and holes were recombined, while others would stay around the valance band and conduction band of CdS and then react with reactants. The band gap energy of CdS was about 2.4 eV, when the CB flat band potential and the VB flat band potential were -1.0 and 1.4 V (*vs* normal hydrogen electrode (NHE), pH = 7)[20]. The excited photoelectron energy in CdS (-1.0V) was more negative than E_0 (CO_2/HCOOH) (-0.61V)[21] and E_0 (CO_2/

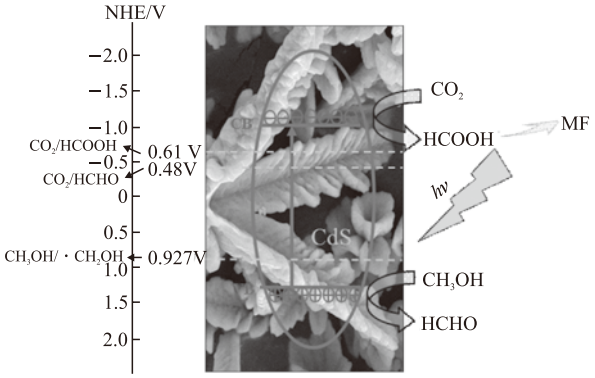

Fig.10 Proposed mechanism for photocatalytically reducing CO_2 over CdS

HCHO) (-0.48V). Thus the photoelectrons could react with CO_2 producing formic acid(HCOOH) or formaldehyde(HCHO). Through the esterification of formic acid and methanol, and dimerization of formaldehyde via Tishchenko reaction[22] MF was produced. The valence band energy in CdS (1.4 V) was more positive than E_0 ($CH_3OH/\cdot CH_2OH$) (0.927 V)[23]. So the vacancies could oxidize CH_3OH to HCHO, and CH_3OH acted as electron donor in this process. The major reaction steps in the process were summarized as the following chemical equations:

Photo excitation of catalyst:

$$CdS \xrightarrow{h\nu} h^+_{VB} + e^- \quad (1)$$

Reactions on conduction band:

$$\begin{aligned} CO_2 + 2e^- + 2H^+ &\longrightarrow HCOOH \\ CO_2 + 4e^- + 4H^+ &\longrightarrow HCHO + H_2O \end{aligned} \quad (2)$$

Reactions on valence band:

$$\begin{aligned} CH_3OH + h_{VB}^+ &\longrightarrow \bullet CH_2OH + H^+ \\ \bullet CH_2OH + h_{VB}^+ &\longrightarrow HCHO + H^+ \end{aligned} \quad (3)$$

Total reactions of generating MF:

$$\begin{aligned} CH_3OH + HCOOH &\longrightarrow HCOOCH_3 + H_2O \\ 2HCHO &\longrightarrow HCOOCH_3 \end{aligned} \quad (4)$$

Neverthless, HCHO was just a intermediate product, and could not be detected by GC. HCHO was further oxidized to HCOOH then producing MF in CH_3OH. This might explain why MF was generated when CO_2 was not bubbled into CH_3OH. Then, through the above analysis of the control experiment, it could be found that the reduction of CO_2 played a key role in the production of MF in methanol. The reaction mechanism expression is showed in Fig.10.

4 Conclusions

a) By changing cadmium source and sulfur source, various of CdS photocatalysts were template-free hydrothermally synthesized with different morphologies, such as microsphere, flower-like, leaf-like and so on.

b) Hydrothermal crystallization time, cadmium source and sulfur source all had great impact on the morphology and photocatalytic activity of the CdS samples. The CdS microsphere samples had better photocatalytic performance than the unique flower-like samples.

c) Only under the influence of the CdS sample synthesized from CadN and TAA, DMM was investigated in the photocatalytic reaction of CO_2 using methanol as reactant and solvent. And the CdS catalysts synthesized from CadN and TAA had the best photocatalytic activity.

References

[1] Li Y, Wang W N, Zhan Z, *et al*. Photocatalytic Reduction of CO_2 with H_2O on Mesoporous Silica Supported Cu/TiO_2 Catalysts[J]. *Applied Catalysis B: Environmental*, 2010, 100: 386-392

[2] Tseng I H, Chang W C, Wu J C S. Photoreduction of CO_2 Using Sol-gel Derived Titania and Titania-supported Copper Catalysts[J]. *Applied Catalysis B: Environmental*, 2002, 37: 37-48

[3] Zhang Q Y, Li Y, Ackerman E A, *et al*. Visible Light Responsive Iodine-Doped TiO_2 for Photocatalytic Reduction of CO_2 to Fuels[J]. *Applied Catalysis A General*, 2011, 400(1): 195-202

[4] Zhao C Y, Krall A, Zhao H L, *et al.* Ultrasonic Spray Pyrolysis Synthesis of Ag/TiO_2 Nanocomposite Photocatalysts for Simultaneous H_2 Production and CO_2 Reduction[J]. *International Journal of Hydrogen Energy*, 2012, 37: 9 967-9 976

[5] Chen J S, Xin F, Qin S Y, *et al.* Photocatalytically Reducing CO_2 to Methyl Formate in Methanol Over ZnS and Ni-doped ZnS Photocatalysts[J]. *Chemical Engineering Journal*, 2013, 230: 506-512

[6] Jiang W L, Yin X H, Xin F, *et al.* Preparation of $CdIn_2S_4$ Microspheres and Application for Photocatalytic Reduction of Carbon Dioxide[J]. *Applied Surface Science*, 2014, 288:138-142

[7] Min Y L, He G Q, Xu Q J, *et al*. Dual-functional MoS_2 Sheet-modified CdS Branch-like Heterostructures with Enhanced Photostability and Photocatalytic Activity[J]. *J. Mater. Chem. A*, 2014, 2: 2 578-2 581

[8] Wang Z, Hou J G, Yang C, *et al*. Three-dimensional MoS_2–CdS–γ-Ta-ON Hollow Composites for Enhanced Visible-light-driven Hydrogen Evolution[J]. *Chemical Communication*, 2014, 50: 1 731-1 734

[9] Wang W Z, Ao L, He G, *et al.* Room Temperature Surfactant-assisted One-step, Solid-State Synthesis of CdS Nanorods[J]. *Materials Letters*, 2008, 62: 1 014-1 017

[10] Chen M H, Kim Y N, Li C C, *et al.* Controlled Synthesis of Hyperbranched Cadmium Sulfide Micro/Nanocrystals[J]. *Crystal Growth Design*, 2008, 8: 629-634

[11] Li Y X, Hu Y F, Peng S Q, *et al*. Synthesis of CdS Nanorods by an Ethylenediamine Assisted Hydrothermal Method for Photocatalytic Hydrogen Evolution[J]. *Journal of Physical Chemistry C*, 2009, 113: 9 352-9 358

[12] Jun Y W, Lee S M, Kang N J, *et al.* Controlled Synthesis of Multi-armed CdS Nanorod Architectures Using Monosurfactant System[J]. *Journal of the American Chemical Society*, 2001, 123: 5 150-5 151

[13] Yong K T, Sahoo Y, Swihart M T, *et al.* Shape Control of CdS Nanocrystals in One-pot Synthesis[J]. *Journal of Physical Chemistry C*, 2007, 111: 2 447-2 458

[14] Wang X L, Fan D Y, Feng Z C, *et al.* Shape-Controlled Synthesis of CdS Nanostructures via Solvothermal Method[J]. *Crystal Growth & Design*, 2010, 10: 5 312-5 318

[15] Xu Y, Schoonen M A A. The Absolute Energy Positions of Conduction and Valence Bands of Selected Semiconducting Minerals[J]. *American Mineralogist*, 2000, 85: 543-556

[16] You Y, Wan L, Zhang S Y, *et al.* Effect of Different Doping Methods on Microstructure and Photo-catalytic Activity of Ag_2O-TiO_2 Nanofibers[J]. *Materials Research Bulletin*., 2010, 45: 1 850-1 854

[17] Sui D D, Yin X H, Dong H Z, *et al*. Photocatalytically Reducing CO_2 to Methyl Formate in Methanol Over Ag Loaded $SrTiO_3$ Nanocrystal Catalysts[J]. *Catalysis Letters*, 2012. 142: 1 202-1 210

[18] Cheng H F, Huang B B, Liu Y Y, *et al.* An Anion Exchange Approach to Bi_2WO_6 Hollow Microspheres with Efficient Visible Light Photocatalytic Reduction of CO_2 to Methanol[J]. *Chemical Communications*, 2012, 48: 9 729-9 731

[19] Nanu M, Schoonman J, Goossens A. Nanocomposite Three-dimensional Solar Cells Obtained by Chemical Spray Deposition[J]. *Nano Letters*, 2005, 5: 1 716-1 719

[20] Tu W, Zhou Y, Zou Z. Photocatalytic Conversion of CO_2 into Renewable Hydrocarbon Fuels: State-of-the-art Accomplishment, Challenges, and Prospects[J]. *Advanced Materials*, 2014, 26: 4 607-4 626

[21] Lehn J M, Ziessel R. Photochemical Generation of Carbon Monoxide and Hydrogen by Reduction of Carbon Dioxide and Water Under Visible Light Irradiation[J]. *Proceedings of the National Academy of Sciences*, 1982, 79(2):701-704

[22] Chung M J, Moon D J, Park K Y, *et al.* Mechanism of Methyl Formation on Cu/ZnO Catalysts[J]. *Journal of Catalysis*, 1992, 136: 609-612

[23] Chen X B, Shen S H, Guo L J, *et al.* Semiconductor-based Photocatalytic Hydrogen Generation[J]. *Chemical Reviews*, 2010, 110: 6 503-6 570